



## Research Article

## SPECIAL ISSUE: Physiology and Ecology of Halophytes—Plants Living in Salt-Rich Environments

Light–dark O<sub>2</sub> dynamics in submerged leaves of C<sub>3</sub> and C<sub>4</sub> halophytes under increased dissolved CO<sub>2</sub>: clues for saltmarsh response to climate changeB. Duarte<sup>1,2\*</sup>, D. Santos<sup>1,2</sup>, H. Silva<sup>3</sup>, J. C. Marques<sup>2,4</sup>, I. Caçador<sup>1,2</sup> and N. Sleimi<sup>5</sup><sup>1</sup> Centre of Oceanography of the Faculty of Sciences, University of Lisbon (CO), Campo Grande, 1749-016 Lisbon, Portugal<sup>2</sup> MARE—Marine and Environmental Sciences Centre, Faculty of Sciences, University of Lisbon, Campo Grande 1749-016 Lisbon, Portugal<sup>3</sup> Biology Department & Centre for Environmental and Marine Studies (CESAM), University of Aveiro, Campus de Santiago, 3810-193 Aveiro, Portugal<sup>4</sup> c/o Department of Zoology, Faculty of Sciences and Technology, Institute of Marine Research—Marine and Environment Research Centre (IMAR-CMA), University of Coimbra, 3000 Coimbra, Portugal<sup>5</sup> UR: MaNE, Faculté des sciences de Bizerte, Université de Carthage, 7021 Jarzouna, Bizerte, Tunisie**Received:** 23 June 2014; **Accepted:** 22 October 2014; **Published:** 7 November 2014**Guest Editor:** Tim J. Flowers**Citation:** Duarte B, Santos D, Silva H, Marques JC, Caçador I, Sleimi N. 2014. Light–dark O<sub>2</sub> dynamics in submerged leaves of C<sub>3</sub> and C<sub>4</sub> halophytes under increased dissolved CO<sub>2</sub>: clues for saltmarsh response to climate change. *AoB PLANTS* 6: plu067; doi:10.1093/aobpla/plu067

**Abstract.** Waterlogging and submergence are the major constraints to which wetland plants are subjected, with inevitable impacts on their physiology and productivity. Global warming and climate change, as driving forces of sea level rise, tend to increase such submersion periods and also modify the carbonate chemistry of the water column due to the increased concentration of CO<sub>2</sub> in the atmosphere. In the present work, the underwater O<sub>2</sub> fluxes in the leaves of two abundant Mediterranean halophytes were evaluated at different levels of dissolved CO<sub>2</sub>. Photosynthetic enhancement due to increased dissolved CO<sub>2</sub> was confirmed for both *Halimione portulacoides* and *Spartina maritima*, probably due to high tissue porosity, formation of leaf gas films and reduction of the oxygenase activity of Rubisco. Enhancement of the photosynthetic rates in *H. portulacoides* and *S. maritima* was concomitant with an increase in energy trapping and transfer, mostly due to enhancement of the carboxylation reaction of Rubisco, leading to a reduction of the energy costs for carbon fixation. Transposing these findings to the ecosystem, and assuming increased dissolved CO<sub>2</sub> concentration scenarios, the halophyte community displays a new ecosystem function, increasing the water column oxygenation and thus reinforcing their role as principal primary producers of the estuarine system.

**Keywords:** Halophytes; PSII photochemistry; rising CO<sub>2</sub>; underwater photosynthesis.

\* Corresponding author's e-mail address: baduarte@fc.ul.pt

Published by Oxford University Press on behalf of the Annals of Botany Company.

This is an Open Access article distributed under the terms of the Creative Commons Attribution License (<http://creativecommons.org/licenses/by/4.0/>), which permits unrestricted reuse, distribution, and reproduction in any medium, provided the original work is properly cited.

## Introduction

Wetlands are among the most productive ecosystems of the planet, retaining about one-half to one-third of the carbon fixed and providing important ecosystem services to the estuarine system, namely nutrient regeneration, primary production and shoreline stabilization as well as a habitat for wildlife (Caçador et al. 2009). Estuarine wetlands are known for their high productivity, which has been attributed to the high degree of halophyte coverage and diversity, with specific zonation, resulting from inter-specific relationships between species and competition for specific optimal habitats (Mendelssohn and Morris 2000). Another key factor defining species expansion, growth and productivity is their exposure to abiotic stresses, both environmental (for example, climate driven) and anthropogenic (for example, pollution with heavy metals). If the future of these ecosystems is to be predicted in the face of climate change, it is of great importance to understand plant stress responses and adaptations at the molecular, biochemical, cellular and physiological levels (Yamaguchi-Shinozaki and Shinozaki 2006; Urano et al. 2010).

Waterlogging and submergence are two major features to which wetland plants, especially salt marsh halophytes, are subjected with severe impacts on their survival and productivity (Bailey-Serres and Voesenek 2008; Pedersen et al. 2010). Due to tidal flooding, shoots and leaves can become completely submerged, restricting gas exchange and light harvesting (Colmer and Voesenek 2009). The frequency, duration and depth of tidal flooding can influence species distribution in salt marshes, this being determined by, for example, their ecophysiological tolerance to flooding (Voesenek et al. 2004; Pedersen and Colmer 2006). Not only does the slow diffusion of CO<sub>2</sub> in the aquatic environment limit its uptake by leaves (Smith and Walker 1980), but also the decreased light availability, due to attenuation down the water column, impairs photosynthesis (Sand-Jensen 1989; Pedersen and Colmer 2006). Several plant species have developed leaf adaptations to these constraints in order to enhance underwater CO<sub>2</sub> uptake by reducing morphologically the boundary layer and cuticle resistance or by acquiring HCO<sub>3</sub><sup>-</sup> directly from the water column (Colmer and Pedersen 2008). In submerged leaves of halophytes, CO<sub>2</sub> limitation becomes severe when concentrations are near air equilibrium, due to the elevated saturation point of underwater photosynthesis (20–75 times the water–air equilibrium conditions; Pedersen et al. 2010). Taking into account the present projections made by the Intergovernmental Panel for Climate Change (IPCC), it is expected that the increased levels of atmospheric CO<sub>2</sub> will lead to an inevitable increase in the

dissolved CO<sub>2</sub> in water bodies (IPCC 2002), in this way altering the availability of CO<sub>2</sub> underwater.

*Spartina maritima* (L.) Loisel (Poaceae) and *Halimione portulacoides* (L.) Allen (Amaranthaceae) are two of the most abundant and productive halophytic plants present in the Mediterranean estuaries (Duarte et al. 2010; Caçador et al. 2013). These species typically colonize the lower marsh mudflats and the sides of the network of channels within the marshes, being subjected to tidal flooding twice per day (Duarte et al. 2009, 2014a). Nevertheless, these are photosynthetically different species: *H. portulacoides* utilizes C<sub>3</sub> photosynthesis (Duarte et al. 2012, 2014b), while *S. maritima* is a C<sub>4</sub> plant (Duarte et al. 2013a, b; Duarte et al. 2014b). Previous work has shown that these species present very different dynamics under atmospheric CO<sub>2</sub> enrichment as well as under submersion (Duarte et al. 2014a, b).

In the present paper, we report the O<sub>2</sub> dynamics in both light-exposed and dark-incubated leaves of C<sub>3</sub> *H. portulacoides* and C<sub>4</sub> *S. maritima* under different dissolved CO<sub>2</sub> concentrations. This has provided insights not only on the species tolerance to submersion but also how CO<sub>2</sub> can ameliorate the imposed submersion stress and its consequences in the ecosystem services provided, namely in terms of water column oxygenation.

## Methods

### Plant harvest

Intact turfs of the target species were collected at the end of the growing season (October), 1 day before the experiments started, from the Tagus estuary (Alcochete, 38°45′38.78″N, 8°56′7.37″W). All the turfs of the same species were of similar height to ensure similar ages. The intact turfs and their rhizosediment were transported to the laboratory of Marine Botany of the Centre of Oceanography, in air-exposed trays and placed in a FytoScope Chamber (Photon Systems Instruments, Czech Republic), in a photoperiod (16/8 h light/dark) at 20 °C, until the beginning of the experiments. Sediment was supplemented with one-fourth strength Hoagland solution with the salinity adjusted to 20 ‰ (estuarine salinity) to maintain moisture conditions from the field.

### Underwater net photosynthesis and respiration

The experimental set-up was based on that of Colmer and Pedersen (2008) for similar experiments. Fully expanded leaves (*n* = 3) were excised from the base of the stem. In the case of *S. maritima* leaves, samples were sliced into similar rectangular segments (~5 cm) by cutting their extremities. For *H. portulacoides*, intact excised leaves were used, as their approximate length was 5 cm. The segments

were immediately placed in 50-mL plastic gas-tight bottles with rubber stoppers (three bottles containing three leaf segments each, per treatment). The Hoagland solution ( $\frac{1}{4}$  strength) was used as the incubation medium with salinity adjusted to 20 ‰ (estuarine salinity) with sea salt mixture and supplemented with KHCO<sub>3</sub> in order to attain the desired dissolved CO<sub>2</sub> levels (0.05, 0.5, 1.0 and 2.0 mM) and the pH adjusted to 6 with KOH, according to field measurements (Duarte et al. 2014c). These four dissolved CO<sub>2</sub> concentrations correspond to 5.0, 50.0, 100 and 200  $\mu\text{M}$  of HCO<sub>3</sub><sup>-</sup>, respectively. Three replicate bottles per treatment were maintained in the light (PAR 400  $\mu\text{mol photons m}^{-2} \text{s}^{-1}$  inside the bottle), while the remaining three replicate bottles were darkened. Both groups were maintained at 25 °C. Bottles containing only the incubation medium were placed under the same conditions to confirm that the O<sub>2</sub> concentrations were maintained constant in the absence of leaves. Underwater net photosynthesis ( $P_N$ ) and respiration ( $R_N$ ) were measured using a dissolved oxygen electrode (WTW Oxi 330i/SET) after 2 h. All tubes were gently stirred every 30 min to allow a homogeneous distribution of oxygen on the incubation medium (Colmer and Pedersen 2008), as confirmed by the constant O<sub>2</sub> values verified in the blank tubes (only Hoagland solution at different levels of dissolved CO<sub>2</sub> without leaves) during the time course. The lack of headspace prevented the escape of gaseous CO<sub>2</sub>. Due to differences in the morphology and succulence of the leaves of the two species, O<sub>2</sub> fluxes were expressed on the basis of dry weight. To determine the dry weight (DW) of the leaves, 20 samples per species, from the same intact turfs used in the experiments, were collected and dried at 60 °C until constant weight and re-weighted. This normalization was adopted instead of using chlorophyll since during stress conditions chlorophyll content can be affected and thus affect the normalization.

In order to achieve a projection of the O<sub>2</sub> production/consumption rates in the Tagus estuarine system, the rates determined in this work were combined with the known biomasses and areas colonized by each of the studied species in the Tagus estuary (Caçador et al. 2009; Duarte et al. 2010; Caçador et al. 2013). The computed values were expressed on a daily basis, considering two high tides per day (one in daytime and another during the night) with a maximum period of plant submersion of 3 h (Serôdio and Catarino 2000; Duarte et al. 2014b). The calculations were made for the four dissolved CO<sub>2</sub> scenarios tested in the present work and the O<sub>2</sub> production/consumption rates obtained experimentally.

### PAM fluorometry

Modulated chlorophyll fluorescence measurements were made in attached leaves in the field with a FluoroPen

FP100 PAM (Photon Systems Instruments). For chlorophyll fluorescence measurements leaves from the light incubations were used. All the measurements in the dark-adapted state were made after covering the leaves with an aluminium foil for 30 min. The minimal fluorescence ( $F_0$ ) in the dark-adapted state was determined using the measuring modulated light, which was sufficiently low ( $<0.1 \mu\text{mol m}^{-2} \text{s}^{-1}$ ) not to induce any significant variation in fluorescence. The maximal fluorescence level ( $F_M$ ) in the dark-adapted state was measured by a 0.8-s saturating pulse at 8000  $\mu\text{mol m}^{-2} \text{s}^{-1}$ . The maximum photochemical efficiency was assessed as  $(F_M - F_0)/F_M$ . The same parameters were also measured in light-adapted leaves, with  $F_0'$  being the minimum fluorescence,  $F_M'$  the maximum fluorescence and the operational photochemical efficiency. Rapid light curves (RLCs) measured in dark-adapted leaves were attained using the pre-programmed LC1 protocol of the FluoroPen, consisting of a sequence of pulses from 0 to 500  $\mu\text{mol m}^{-2} \text{s}^{-1}$ . During this protocol, the  $F_0$  and  $F_M$  as well as the maximum photochemical efficiency were measured. Each  $\Phi\text{PSII}$  measurement was used to calculate the electron transport rate (ETR) through Photosystem II (PSII) using the following equation:  $\text{ETR} = \Phi\text{PSII} \times \text{PAR} \times 0.5$ , where PAR is the actinic photosynthetically active radiation generated by the FluoroPen and 0.5 assumes that the photons absorbed are equally partitioned between PSII and PSI (Genty et al. 1989). Without knowledge of the actual amount of light being absorbed, fluorescence measurements can only be used as an approximation for electron transport (Beer et al. 1998a, b; Runcie and Durako 2004). Rapid light curves were generated from the calculated ETRs and the irradiances applied during the RLC steps. Each RLC was fitted to a double exponential decay function in order to quantify the characteristic parameters,  $\alpha$  and  $\text{ETR}_{\text{max}}$  (Platt et al. 1980). The initial slope of the RLC ( $\alpha$ ) is a measure of the light-harvesting efficiency of photosynthesis and the asymptote of the curve and the maximum rate of photosynthesis ( $\text{ETR}_{\text{max}}$ ) is a measure of the capacity of the photosystems to utilize the absorbed light energy (Marshall et al. 2000). The onset of light saturation ( $E_k$ ) was calculated as the ratio between  $\text{ETR}_{\text{max}}$  and  $\alpha$ . Excitation light of 650 nm (peak wavelength) from an array of three light-emitting diodes was focused on the surface of the leaf to provide a homogeneous illumination. Light intensity reaching the leaf was 3000  $\mu\text{mol m}^{-2} \text{s}^{-1}$ , which was sufficient to generate maximum fluorescence in all individuals. The fluorescence signal is received by the sensor head during recording and is digitized in the control unit using a fast digital converter. The OJIP transient (or Kaustsy curves) depicts the rate of reduction kinetics of various components of PS II. When a dark-adapted leaf is illuminated

with a saturating light intensity of 3500  $\mu\text{mol m}^{-2} \text{s}^{-1}$ , it exhibits a polyphasic rise in fluorescence (OJIP). Each letter reflects distinct inflection in the induction curve. The level O represents all the open reaction centres (RC) at the onset of illumination with no reduction of QA (fluorescence intensity lasts for 10 ms). The rise of transient from O to J indicates the net photochemical reduction of QA (the stable primary electron acceptor of PS II) to QA<sup>-</sup> (lasts for 2 ms). The phase from J to I was due to all reduced states of closed RCs such as QA<sup>-</sup> QB<sup>-</sup>, QA QB<sup>2-</sup> and QA<sup>-</sup> QB H<sub>2</sub> (lasts for 2–30 ms). The level P (300 ms) coincides with maximum concentration of QA<sup>-</sup> QB<sub>2</sub> with the maximally reduced plastoquinol pool. Phase P also reflects a balance between the light incident at the PS II side and the rate of utilization of chemical (potential) energy and the rate of heat dissipation

(Zhu et al. 2005). From this analysis several photochemical parameters were attained and are summarized in Table 1.

### Antioxidant enzymatic activities

All enzyme extraction procedures were performed at 4 °C. Briefly, fresh leaves were homogenized in sodium phosphate buffer (50 mM, pH 7.6) with Na-EDTA (0.1 mM) at a ratio of 8 mL per 500 mg fresh weight. The homogenate was centrifuged at 8923 rpm for 20 min, at 4 °C, and the supernatant was used for the enzymatic assays. Enzymatic activity measurements were performed at room temperature (18 °C).

Catalase (CAT) activity was measured according to the method of Teranishi et al. (1974) by monitoring the consumption of H<sub>2</sub>O<sub>2</sub> and consequent decrease in

**Table 1.** Summary of fluorometric analysis parameters and their description. NPQ, non-photochemical quenching.

<i>PSII efficiency</i>	
$F'_0$ and $F_0$	Basal fluorescence under weak actinic light in light- and dark-adapted leaves
$F'_M$ and $F_M$	Maximum fluorescence measured after a saturating pulse in light- and dark-adapted leaves
$F'_V$ and $F_V$	Variable fluorescence light ( $F'_M - F'_0$ ) and dark ( $F_M - F_0$ )-adapted leaves
PSII operational and maximum quantum yield	Light- and dark-adapted quantum yield of primary photochemistry, equal to the efficiency by which an absorbed photon trapped by the PSII reaction centre will result in the reduction of $Q_A$ to $Q_A^-$
NPQ	
RLCs	
rETR	Relative ETR at each light intensity ( $\text{rETR} = \text{QY} \times \text{PAR} \times 0.5$ )
$\alpha$	Photosynthetic efficiency, obtained from the initial slope of the RLC
<i>OJIP-derived parameters</i>	
$\psi_{P0}$	Maximum yield of primary photochemistry
$\psi_{E0}$	Probability that an absorbed photon will move an electron into the ETC
$\psi_{D0}$	Quantum yield of the non-photochemical reactions
$\varphi_0$	Probability of a PSII-trapped electron to be transported from $Q_A$ to $Q_B$
$P_G$	Grouping probability is a direct measure of the connectivity between the two PSII units (Strasser and Stirbet 2001)
ABS/CS	Absorbed energy flux ( $F_0$ )
TR <sub>0</sub> /CS	Trapped energy flux ( $\text{ABS/CS} \times \psi_{P0}$ )
ET <sub>0</sub> /CS	Electron transport energy flux ( $\psi_{P0} \times \varphi_0 \times \text{ABS/CS}$ )
DI <sub>0</sub> /CS	Dissipated energy flux ( $\text{ABS/CS} - \text{TR}_0/\text{CS}$ )
Diving force for photosynthesis (DF ABS)	$\text{DF ABS} = \text{DF RC} + \text{DF } (\psi_{P0} + \text{DF } \varphi)$
Driving force for trapping electronic energy (DF $\psi_{P0}$ )	$\text{DF } \psi_{P0} = \log (\psi_{P0}/(1 - \psi_{P0}))$
Driving force for electron transport (DF $\varphi$ )	$\text{DF } \varphi = \log (\varphi_0/(1 - \varphi_0))$
Driving force for energy absorption (DF RC)	$\text{DF RC} = \log (\text{RC/ABS})$



absorbance at 240 nm. ( $\epsilon = 39.4 \text{ mM}^{-1} \text{ cm}^{-1}$ ). The reaction mixture contained sodium phosphate buffer (50 mM, pH 7.6), Na-EDTA (0.1 mM) and H<sub>2</sub>O<sub>2</sub> (100 mM). The reaction was started with the addition of the extract. Ascorbate peroxidase was assayed according to Tiryakioglu et al. (2006). The reaction mixture contained sodium phosphate buffer (50 mM, pH 7.0), H<sub>2</sub>O<sub>2</sub> (12 mM) and L-ascorbate (0.25 mM). The reaction was initiated with the addition of 100  $\mu\text{L}$  of the enzyme extract. The activity was recorded as the decrease in absorbance at 290 nm, and the amount of ascorbate oxidized was calculated from the molar extinction coefficient of  $2.8 \text{ mM}^{-1} \text{ cm}^{-1}$ .

Guaiacol peroxidase was measured by the method of Bergmeyer et al. (1974) with a reaction mixture consisting of sodium phosphate buffer (50 mM, pH 7.0), H<sub>2</sub>O<sub>2</sub> (2 mM) and guaiacol (20 mM). The reaction was initiated with the addition of 100  $\mu\text{L}$  of the enzyme extract. The enzymatic activity was measured by monitoring the increase in absorbance at 470 nm ( $\epsilon = 26.6 \text{ mM}^{-1} \text{ cm}^{-1}$ ).

Superoxide dismutase (SOD) activity was assayed according to Marklund and Marklund (1974) by monitoring the reduction of pyrogallol at 325 nm. The reaction mixture contained sodium phosphate buffer (50 mM, pH 7.6), Na-EDTA (0.1 mM), pyrogallol (3 mM) and Milli-Q water. The reaction was started with the addition of 10  $\mu\text{L}$  of the enzyme extract. Control assays were done in the absence of a substrate in order to evaluate the auto-oxidation of the substrates.

All enzymatic activities were expressed as U  $\mu\text{g}^{-1}$  of protein, where U, a unit, is the amount of enzyme that catalyses the conversion of 1  $\mu\text{mol}$  of substrate per second.

Proteins were determined according to Bradford (1976), using bovine serum albumin as the standard protein.

## Statistical analysis

In order to compare the results of the different ecophysiological parameters between species at different treatments, the Kruskal–Wallis test was employed. Statistical analyses were carried out using the Statistica Software version 10 (StatSoft).

## Results

### Underwater net photosynthesis and respiration

For *H. portulacoides*, an increase in dissolved CO<sub>2</sub> led to an increase in O<sub>2</sub> production (photosynthesis) in the light-exposed leaves and a decrease in the O<sub>2</sub> consumption (respiration) with increasing dissolved CO<sub>2</sub> concentrations in dark-incubated leaves (Fig. 1). For *S. maritima*, however, increased dissolved CO<sub>2</sub> leads to a decrease in O<sub>2</sub> consumption rates (respiration) in light-exposed leaves. In fact, underwater photosynthetic O<sub>2</sub> production could only be observed under higher dissolved CO<sub>2</sub> concentrations. Regarding the dark-adapted leaves of *S. maritima*, there was no distinct pattern of variation in O<sub>2</sub> consumption rates with change of dissolved CO<sub>2</sub> concentrations. The highest underwater O<sub>2</sub> production ( $4 \mu\text{mol O}_2 \text{ g}^{-1} \text{ DW h}^{-1}$ ) was recorded in *H. portulacoides* at 0.5 mM dissolved CO<sub>2</sub>, while *S. maritima* showed the lowest ( $1.6 \mu\text{mol O}_2 \text{ g}^{-1} \text{ DW h}^{-1}$ ) even at elevated dissolved CO<sub>2</sub> concentrations (2 mM). On the other hand, *S. maritima* exhibited the highest respiratory rates (O<sub>2</sub> consumption

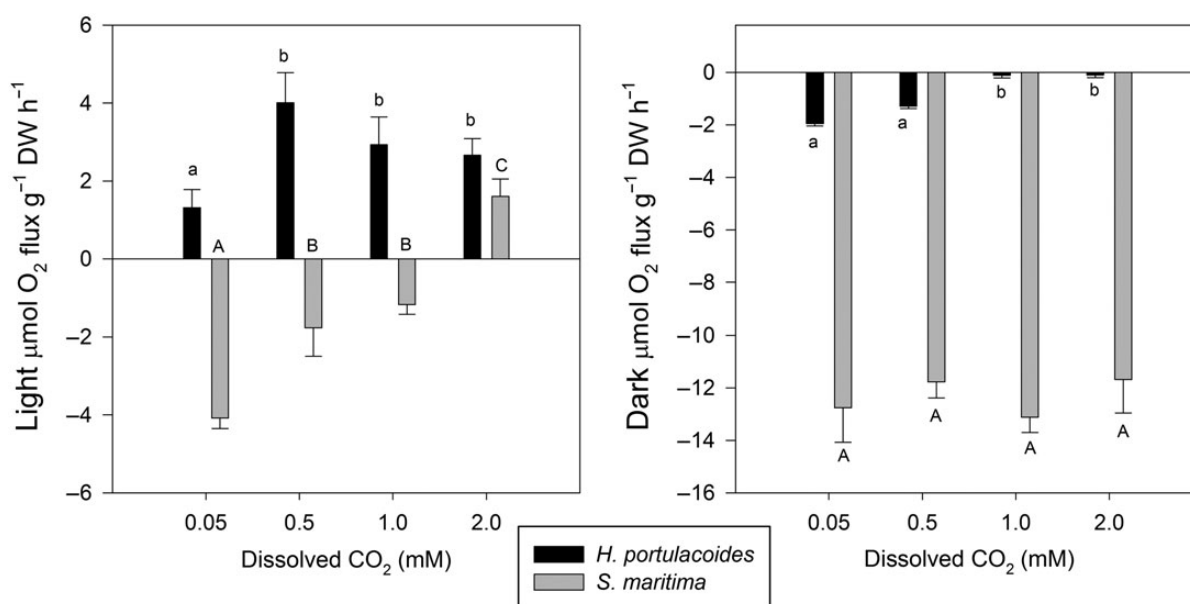


**Figure 1.** Oxygen production and consumption by the two tested species under light and dark conditions, at different levels of dissolved CO<sub>2</sub> (average  $\pm$  standard deviation,  $n = 9$ ). Letters indicate significant differences among CO<sub>2</sub> treatments at  $P < 0.05$ .

in the dark), independently of the applied dissolved CO<sub>2</sub> concentration.

### PAM fluorometry

**PSII quantum efficiencies and variable fluorescence.** The maximum PSII quantum efficiencies (dark-adapted leaves) showed no evident differences among the dissolved CO<sub>2</sub> treatments for either species tested (Fig. 2). As for the operational PSII quantum efficiencies, there was a tendency for reduction with increasing dissolved CO<sub>2</sub> concentrations. The variable fluorescence ( $F_v$ ) in both dark- and light-adapted leaves of *H. portulacoides* showed a decrease in both with increasing CO<sub>2</sub> treatments,

presenting a maximum at 0.5 mM dissolved CO<sub>2</sub>. On the other hand, in *S. maritima* the  $F_v$  in dark-adapted leaves showed an evident increase along with increasing dissolved CO<sub>2</sub> concentrations. Nevertheless, there was no distinguishing pattern in the variable fluorescence data in light-adapted leaves of *S. maritima*.

**Kautsky curves and transient OJIP parameters.** The O–J phase of the Kautsky curves of all samples presented similar patterns, independently of the dissolved CO<sub>2</sub> concentrations (Fig. 3). In *H. portulacoides*, the more evident differences were observed during the thermal phase (J–I–P), with higher values in the samples exposed to higher dissolved

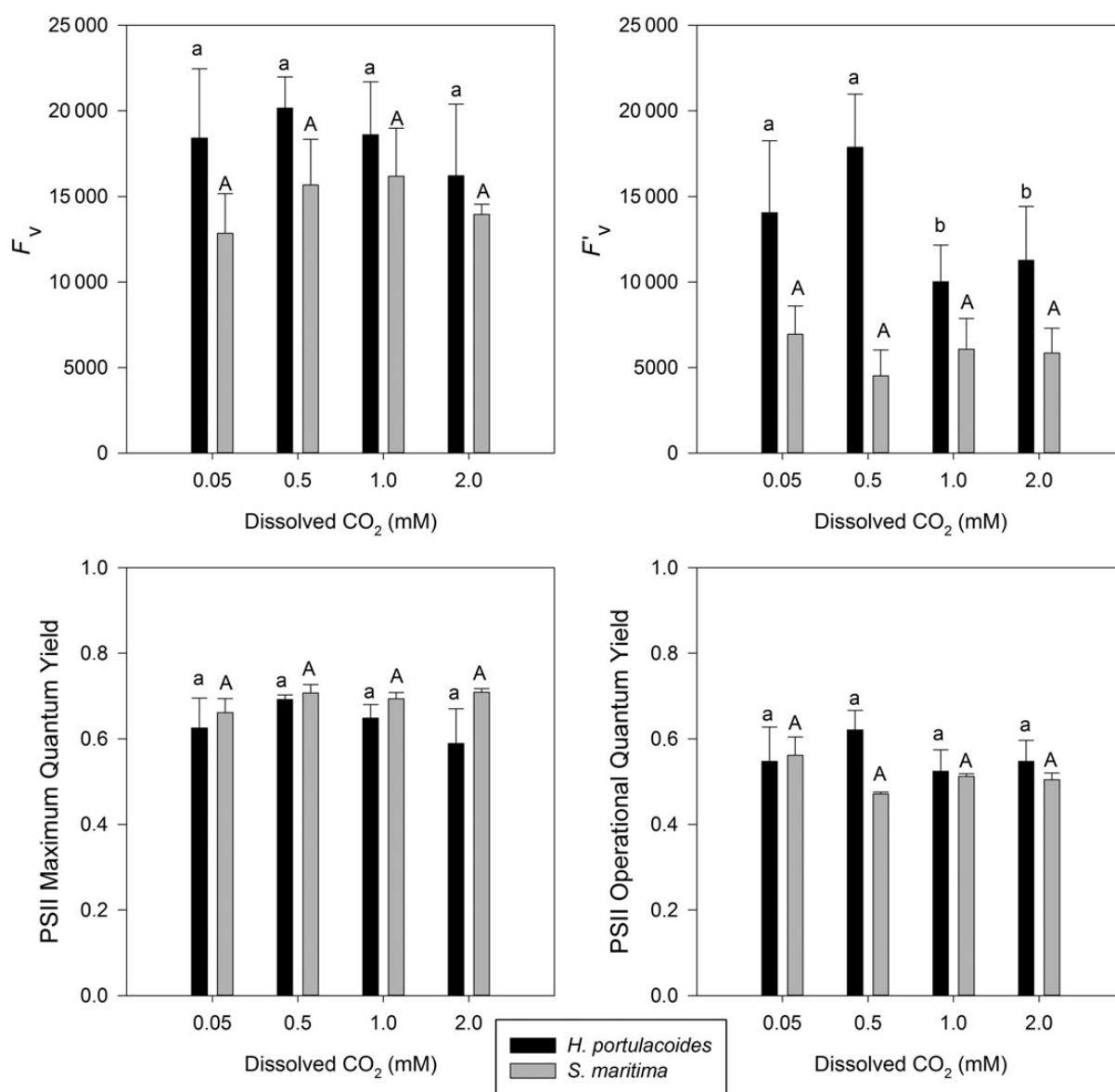


**Figure 2.** Photosystem II variable fluorescence and quantum efficiencies (operational and maximum) by the two tested species under light and dark conditions, at different levels of dissolved CO<sub>2</sub> (average  $\pm$  standard deviation,  $n = 9$ ). Letters indicate significant differences among CO<sub>2</sub> treatments at  $P < 0.05$ .

CO<sub>2</sub> concentrations. During the photochemical phase (O–J), there was generally an overlap of the Kautsky plots among treatments. For *S. maritima* leaves, the increase in dissolved CO<sub>2</sub> leads to an increase in the intensity of both the photochemical and thermal phases, the latter being more pronounced in leaves subjected to the higher concentration of dissolved CO<sub>2</sub>.

Regarding the OJIP-derived photochemical parameters, as well as the energy flux variables, some differences were evident (Figs 3 and 4). The maximum quantum yield of primary PSII photochemistry ( $\phi_{P0}$ ) was generally maintained both among CO<sub>2</sub> treatments and species. On the other hand, in *H. portulacoides*, small fluctuations were observed in the probability of a PSII trapped electron

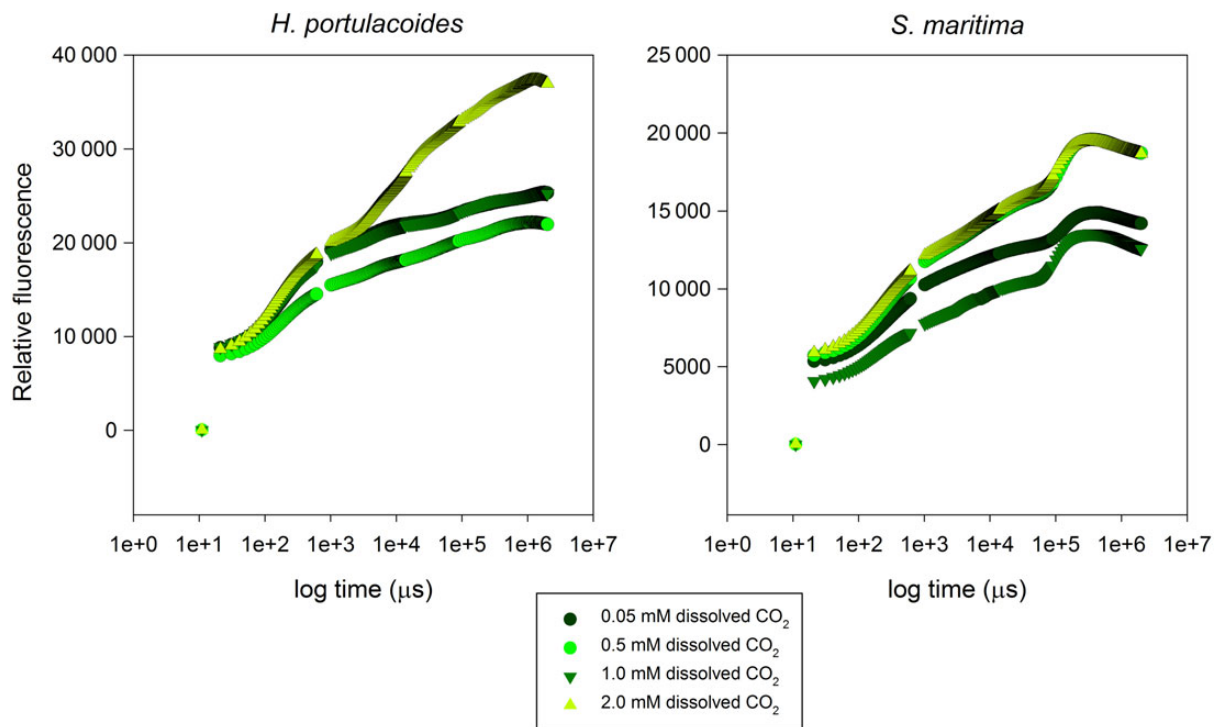


**Figure 3.** Kautsky OJIP curves of the two tested species under light and dark conditions, at different levels of dissolved CO<sub>2</sub> (average,  $n = 9$ ).

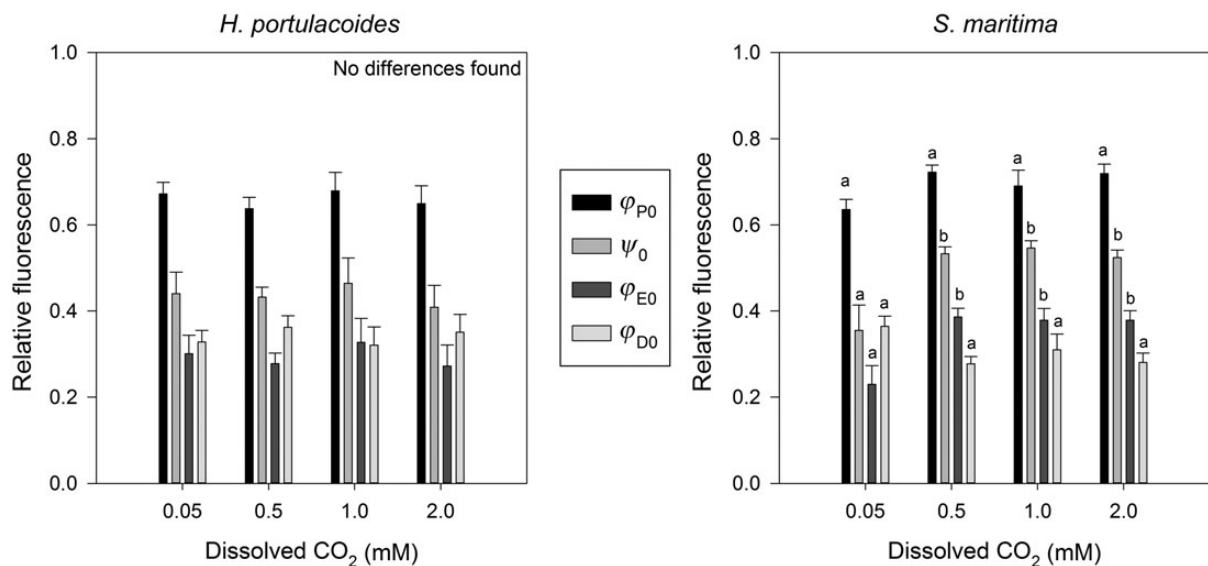


**Figure 4.** OJIP-driven photochemical parameters in the two tested species under light and dark conditions, at different levels of dissolved CO<sub>2</sub> (average  $\pm$  standard deviation,  $n = 9$ ). Letters indicate significant differences among CO<sub>2</sub> treatments at  $P < 0.05$ .

being transferred from QA to QB ( $\psi 0$ ) as well as in the electronic transport quantum yield ( $\varphi Eo$ ) across the different applied CO<sub>2</sub> treatments. With *S. maritima* both parameters showed an increase in their relative fluorescence with increasing dissolved CO<sub>2</sub>. The quantum yield of the non-photochemical reactions ( $\varphi Do$ ) decreased only in *S. maritima* with increasing CO<sub>2</sub>.

If the variations in driving forces at various concentrations of dissolved CO<sub>2</sub> are analysed (Fig. 5), *H. portulacoides* and *S. maritima* showed a decrease in the driving force for photosynthesis (DF<sub>ABS</sub>) mainly due to a decrease in the trapping (DF $\psi$ ) of excitation energy and in the conversion of this excitation energy into electron transport (DF $\varphi$ ). The DF<sub>RC</sub> (light energy absorption) was not affected by the increase in dissolved CO<sub>2</sub>, in both these species. Nevertheless in *H. portulacoides*, there was a recovery of the DF<sub>ABS</sub> at the highest CO<sub>2</sub> level, driven by a simultaneous increase in both DF $\psi$  and DF $\varphi$ .

Normalizing the data on a leaf cross-section basis provided new insights (Fig. 6). It was possible to see that neither of the species presented differences in the number of available PSII RC for light harvesting (RC/CS), or the absorbed (ABS/CS) or trapped (TR/CS) energy fluxes. On the other hand, the energy fluxes for electron transport (ET/CS) in *S. maritima* showed a marked increase upon CO<sub>2</sub> supplementation, while *H. portulacoides* leaves did not show any significant difference in this parameter

or in the dissipated energy fluxes (DI/CS). *Spartina maritima*, on the other hand, showed a marked reduction in the dissipated energy values at above-ambient CO<sub>2</sub> concentrations. This analysis also provided insights on the connectivity between the PSII antennae and thus the PSII-harvesting efficiency (PG). While in *H. portulacoides* the increase of the antennae connectivity only occurred at the highest tested CO<sub>2</sub> concentrations, in *S. maritima* this could be observed in all CO<sub>2</sub> levels above ambient concentrations.

### Antioxidant enzymatic activities

Antioxidant enzymatic defences are presented in Fig. 7. *Halimione portulacoides* showed a marked increase in both CAT and SOD activities with increasing dissolved CO<sub>2</sub> supply and in *S. maritima* leaves there was a decreasing trend in APx and GPx activities along with increasing dissolved CO<sub>2</sub>. Superoxide dismutase activity increased at the highest dissolved CO<sub>2</sub> concentration.

### (De)Oxygenation of the water column

Considering the biomass values per square metre and the total abundance of each of the analysed species, the underwater oxygen consumption/production rates were calculated per square metre on a daily basis, for four tested scenarios (Table 2). It was possible to calculate that *S. maritima* was responsible for the highest O<sub>2</sub> consumptions in the estuarine system. On the other hand,

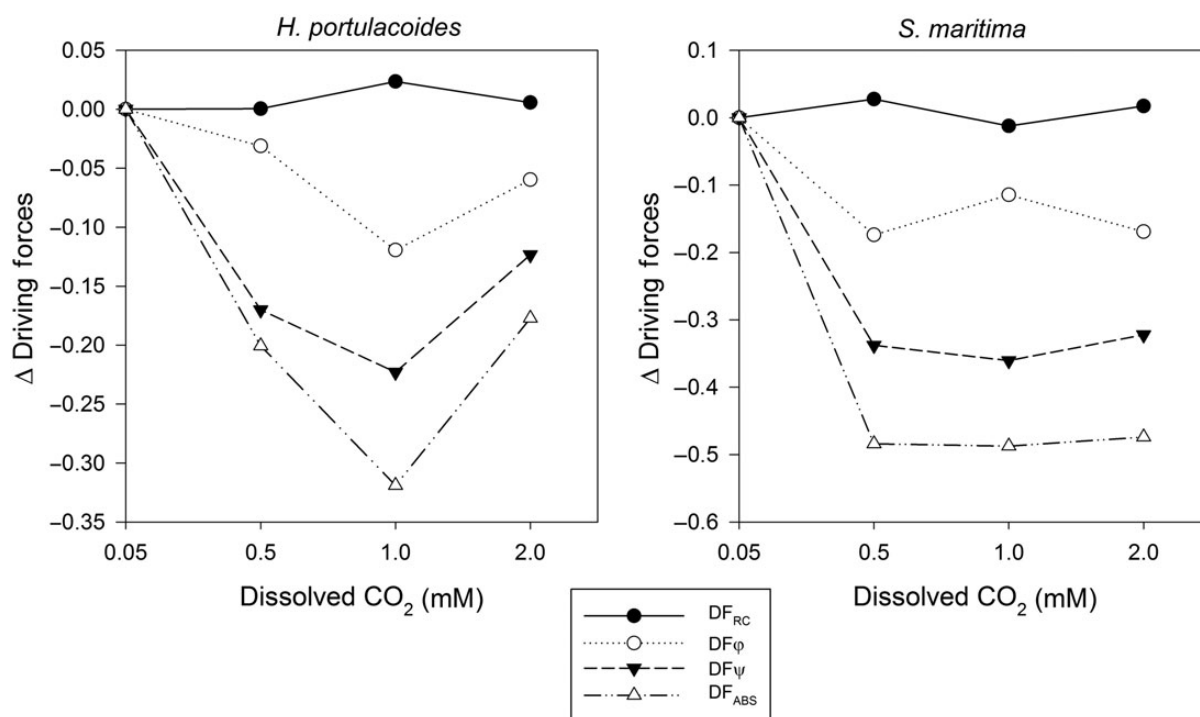


**Figure 5.** Photochemical reactions driving forces in the two tested species under light and dark conditions, at different levels of dissolved CO<sub>2</sub> (average,  $n = 9$ ).



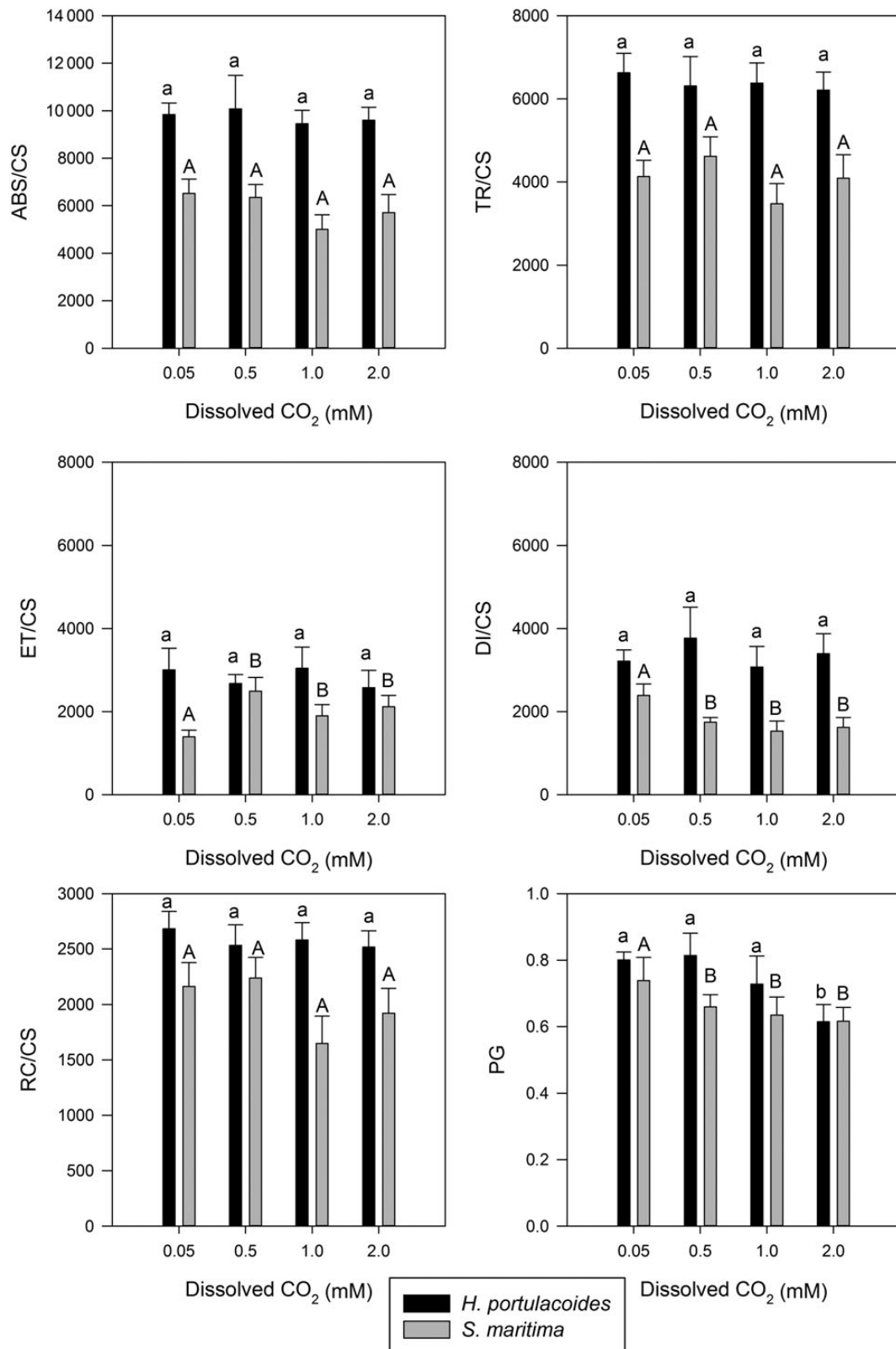


**Figure 6.** Photosystem II antennae connectivity (PG) and energy fluxes on a leaf cross-section basis, in the leaves of the two tested species under light and dark conditions, at different levels of dissolved CO<sub>2</sub> (average  $\pm$  standard deviation,  $n = 9$ . Letters indicate significant differences among CO<sub>2</sub> treatments at  $P < 0.05$ ).

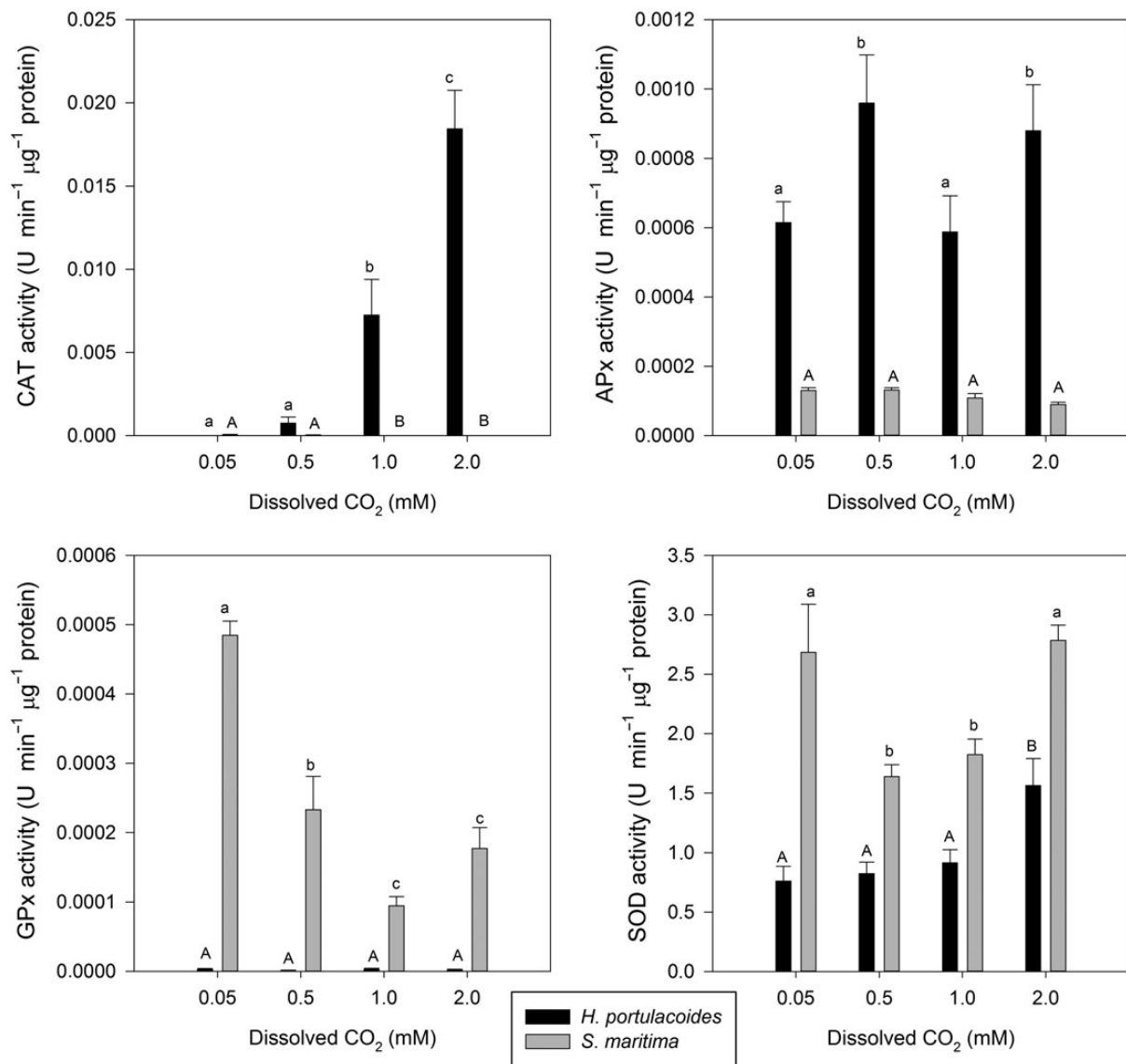


**Figure 7.** Peroxidase (CAT, APx and GPx) and superoxide dismutase (SOD) activity in the leaves of the two tested species under light and dark conditions, at different levels of dissolved CO<sub>2</sub> (average ± standard deviation, *n* = 9. Letters indicate significant differences among CO<sub>2</sub> treatments at *P* < 0.05).

**Table 2.** O<sub>2</sub> (mol) produced (+)/consumed (–) by each halophyte (considering all the coverage area in the Tagus estuary) at the four considered scenarios per day (including light and dark fluxes).

	Dissolved CO <sub>2</sub> concentration (mM)			
Daytime	0.05	0.5	1	2
<i>H. portulacoides</i>	3952 ± 1397	12 050 ± 1397	8816 ± 2140	7990 ± 1301
<i>S. maritima</i>	–2039 ± 135	–879 ± 368	–590 ± 124	801 ± 224
Night	0.05	0.5	1	2
<i>H. portulacoides</i>	–5872 ± 196	–3882 ± 193	–316 ± 224	–297 ± 210
<i>S. maritima</i>	–6379 ± 465	–5885 ± 214	–6557 ± 207	–5840 ± 449
Daily budget	0.05	0.5	1	2
	–10 338	1404	1353	2654

*H. portulacoides* appears as the major contributor for water column oxygenation, with high rates of O<sub>2</sub> production and very low rates of respiration during nighttime. Overall at the community level, as represented by these two species, an increase in dissolved CO<sub>2</sub> concentrations in the water column tended to increase the oxygenation of the water column by these halophytes.

## Discussion

Aquatic plants submerged in different coastal ecosystems are often flooded by water with CO<sub>2</sub> concentrations above the air–water equilibrium (Sand-Jensen et al. 1992; Keeley 1998; Ram et al. 1999; Pedersen et al. 2010; Duarte et al. 2014b). The dissolved CO<sub>2</sub> concentration is a key factor, as its availability controls underwater net photosynthesis, in both terrestrial and aquatic plants (Sand-Jensen et al. 1992; Colmer and Pedersen 2008). In estuaries populated with halophytes, not only is their growth controlled by dissolved CO<sub>2</sub>, but also their function as oxygen providers/consumers. The tolerance of these plants to submersion has often been described on the basis of a quiescence response—the lack of shoot elongation conserves carbohydrates during submersion periods (Bailey-Serres and Voesenek 2008). At night-time an increased O<sub>2</sub> deficit arises as another stressor in submerged conditions, due to the plants' dependency on dissolved O<sub>2</sub> entry from floodwaters for night respiration (Waters et al. 1989; Pedersen and Colmer 2006; Pedersen et al. 2009).

In the present study, two of the more abundant halophytic species in the Portuguese estuarine ecosystems showed very different feedbacks to increases in dissolved CO<sub>2</sub>. The photosynthetic enhancement due to increased dissolved CO<sub>2</sub>, verified for *H. portulacoides* and *S. maritima*, has already been described for rice and for *Hordeum marinum* (Setter et al. 1989; Pedersen et al. 2010). These authors suggested that enhancement was driven by the presence of gas films on the leaf surface and high tissue porosity, allowing higher rates of gas exchange according to CO<sub>2</sub> availability (Pedersen et al. 2010). Also, an increase in [CO<sub>2</sub>]/[O<sub>2</sub>] ratio can improve CO<sub>2</sub>-use efficiency, due to a reduction in Rubisco oxygenase activity (Lorimer 1981; Bowes 1993; Andersen and Pedersen 2002). Although this enhancement was detected even at low dissolved CO<sub>2</sub> concentrations in *H. portulacoides*, for *S. maritima* it was only achieved at high CO<sub>2</sub> concentrations. *Spartina maritima* proved to be highly adapted to submersion, in line with a recent study that also demonstrated the plasticity of *S. maritima* as an efficient adaptation to flooding, allowing plants to recover quickly from the stress imposed by this condition (Duarte et al. 2014b). Being a C<sub>4</sub> species,

these results for *S. maritima* point to a reduction in the oxygenase activity of Rubisco as a consequence of the extremely high internal [CO<sub>2</sub>]/[O<sub>2</sub>]; this, together with a high resistance to CO<sub>2</sub> entry, restricts underwater photosynthesis (Lorimer 1981; Bowes 1993; Andersen and Pedersen 2002). Although *S. maritima* has a high specific leaf area compared with *H. portulacoides*, the presence of a thicker cuticle is probably the factor responsible for this reduced diffusion underwater (Mommer et al. 2007). In *S. maritima*, the CO<sub>2</sub> concentration mechanism occurs in the mesophyll cells catalysed by PEPc supplying the bundle sheath with C<sub>4</sub> organic acids, independently of the O<sub>2</sub> concentration. In sum, C<sub>4</sub> plants with their Kranz anatomy rely on the preferential assimilation of HCO<sub>3</sub><sup>−</sup> (Raven 1970, 1972). Additionally, it should be noted that, under submersion in turbid water, mitochondrial respiration must be included as a possible contributor for O<sub>2</sub> budgets. Nevertheless, under these conditions, *S. maritima* HCO<sub>3</sub><sup>−</sup>-pump allowed an enhancement of the photosynthetic O<sub>2</sub> production at HCO<sub>3</sub><sup>−</sup> concentrations as low as 200 μM. Thus, the CO<sub>2</sub> concentration mechanism in *S. maritima* is apparently highly adapted to underwater conditions, as shown previously (Duarte et al. 2014b), needing comparatively low HCO<sub>3</sub><sup>−</sup> concentrations to efficiently supply the bundle sheath cells with the required CO<sub>2</sub> concentration for restarting the Calvin cycle. On the other hand, C<sub>3</sub> plants depend on the availability of CO<sub>2</sub>, and therefore on the leaf gas film formation (Raven 1970, 1972). The presence of wax-rich cuticles has been reported in hydrophobic leaves of *H. portulacoides* (Grossi and Raphel 2003) and can result in an improvement in gas film formation at the leaf surface, thus promoting gas exchange (Setter et al. 1989; Wagner et al. 2003; Colmer and Pedersen 2008). Nevertheless, the C<sub>3</sub> mechanism of *H. portulacoides*, dependent on the CO<sub>2</sub> acquisition, only showed a significant enhancement at 0.5 mM CO<sub>2</sub> concentration, making it less efficient than the C<sub>4</sub> of *S. maritima*. All these facts indicate that, while underwater, these species are C<sub>i</sub>-limited at normal inorganic carbon concentration in estuarine water.

Alongside the anatomical differences, the photosynthetic and electronic processes showed marked differences in light-harvesting and processing mechanisms. One important fluorescence parameter, normally associated with stress conditions is the variable fluorescence (*F<sub>v</sub>*). The maximum photosynthetic O<sub>2</sub> production in *H. portulacoides*, verified at 0.5 mM dissolved CO<sub>2</sub>, also showed the highest value of *F<sub>v</sub>*, an indicator of low stress conditions (Duarte et al. 2012). The same was true, but to a smaller extent, for the operational quantum yield of this species.

Since CO<sub>2</sub> and O<sub>2</sub> compete for the same Rubisco active sites (Taiz and Zeiger 2002), favouring the carboxylation process and reduction of the oxygenation capacity of Rubisco also implies a decrease in the energy costs for CO<sub>2</sub> fixation and a consequent increase in PSII quantum yield for photosynthesis (Furbank 1998; Taiz and Zeiger 2002). This was confirmed by analysing the principal driving forces underlying the electronic photosynthetic processes. In *H. portulacoides* and *S. maritima* there was not only an increase in the driving forces related to the trapping of excitation energy, but also in transfer of this energy to the electron transport chain. Both these increases lead to an enhancement in total driving force for photosynthesis. It was also interesting to note that, in both species, there were no changes in the light energy absorption ability, confirming the above-mentioned hypothesis (increased PSII efficiency induced by higher Rubisco carboxylation rates) and pointing to an increase in photosynthetic activity due to higher CO<sub>2</sub> availability. In fact, in *S. maritima* this was related to an increase in the probability of a PSII trapped electron being transferred from QA to QB ( $\psi_0$ ) as well as for the quantum yield of this transport between quinones ( $\phi_{Eo}$ ).

All these findings are confirmed by the analysis of the energy fluxes on a cross-sectional area basis. Both species maintained their number of available PSII RC constants and thus the absorbed and trapped energy fluxes did not suffer any changes. Differences arise if the integrity of the PSII antennae is observed and are the basis of the increased energy processing efficiency observed in *S. maritima* leaves. This parameter accounts for all the energetic communication pathways between neighbour PSII antennae (Strasser and Stirbet 2001; Panda et al. 2006). On the contrary to what has been observed in other terrestrial plants, there was no loss of connectivity between the antennae of the PSII units during submersion, indicating an improved survival strategy for underwater conditions (Panda et al. 2006; Duarte et al. 2014b). The increased PSII antennae integrity in *S. maritima* leads to an enhanced efficiency in transporting energy and thus reduction of the dissipated energy. Although this was also noticed in *H. portulacoides* leaves subjected to the highest dissolved CO<sub>2</sub> concentrations tested, it did not result in a significant improvement of the energy fluxes use efficiency, indicating that the increasing dissolved CO<sub>2</sub> concentrations do not affect *H. portulacoides* leaves at the energy processing but in deeper processes.

Comparing the data on antioxidant enzymatic activities with the data from the oxygen production, *H. portulacoides* showed a maximum photosynthetic O<sub>2</sub> production at 0.5 mM CO<sub>2</sub> decreasing towards higher CO<sub>2</sub> concentrations, concomitantly with an increase in CAT activity. This O<sub>2</sub> production decreased or increased consumption

during daytime conditions as well as increased CAT activity, which is in agreement with photorespiratory activation. It is known that activation of photorespiration is an important part of the abiotic stress feedback as a means to dissipate the excessive energy trapped (Voss et al. 2013). With the activation of this mechanism, H<sub>2</sub>O<sub>2</sub> is generated and scavenged by the increased CAT activity. In fact, looking at the data from the principal driving forces, the increase in CAT activity appears simultaneously with a decrease in the driving forces for trapping excitation energy and for photosynthesis. In the C<sub>4</sub> *S. maritima*, peroxidase activity (APx and GPx) showed a concomitant decrease along with the increase in O<sub>2</sub> production. On the other hand, SOD showed two marked peaks driven by distinct and opposite mechanisms. The first peak at 0.05 mM CO<sub>2</sub> is concomitant with high respiratory activity and increased non-photochemical activity, indicating a need to dissipate excessive photon energy, due to the Ci limitation, similar to that observed in plants exposed to increased atmospheric CO<sub>2</sub> (Geissler et al. 2009; Duarte et al. 2014a). The second observed SOD peak, observed in individuals exposed to 2 mM dissolved CO<sub>2</sub>, is coincident with the increase in the photosynthetic activity, and consequent superoxide radical production (Taiz and Zeiger 2002).

Nevertheless, previous studies (Duarte et al. 2014a) with CO<sub>2</sub>-enriched air showed a very different trend, pointing to different stress mechanisms, occurring during submersion. While the C<sub>3</sub> *H. portulacoides* showed an enhancement of the photosynthetic rates while exposed to atmospheric CO<sub>2</sub> enrichment, the same was not observed for the C<sub>4</sub> *S. maritima*. In the present study, this grass showed a very significant improvement in its photosynthetic rates upon dissolved CO<sub>2</sub> fertilization that was not observed in immersed conditions (Duarte et al. 2014b). This points to two interesting aspects: (i) *S. maritima* is probably C<sub>i</sub> limited under submersed conditions and (ii) CO<sub>2</sub> in fact ameliorates the stress imposed by submersion (Duarte et al. 2014a).

All these ecophysiological responses have their repercussions for the ecosystem services provided by the salt marshes, namely in terms of O<sub>2</sub> and CO<sub>2</sub> production for the water column. Considering the average temperature used in these experiments and the biomass production drawn from the literature (Caçador et al. 2009; Duarte et al. 2010) as well as the species coverage (Caçador et al. 2013), a very simple and basic extrapolation was made for the Tagus estuary salt marshes. It was possible to calculate that there is a general trend for increasing water column oxygenation during the daily tidal cycle (two tides, one in the daytime and another during the night-time), driven by plant underwater photosynthesis. This becomes of great importance if we consider salt

marshes as one of the most important primary producers in an estuarine system (Caçador et al. 2007, 2013; Duarte et al. 2010). Oxygen production by the halophytes becomes a key player overcoming the low rates of air–water O<sub>2</sub> diffusion, and thus introduces important amounts of oxygen required for the heterotrophic species (fishes, macro-invertebrates and bacteria). According to this conclusion, a new saltmarsh service arises as a crucial O<sub>2</sub> producer for the estuarine aquatic community to accompany the role of these marshes as important carbon-harvesting primary producers.

## Conclusions

The diurnal tidal flooding imposes on the halophyte community an underwater environment where gas concentrations are very different from the atmospheric ones. The predicted atmospheric CO<sub>2</sub> increase will have consequences not only on the atmospheric composition, but also on the carbonate chemistry of estuarine water. It is important to consider the physiology of each species, and the consequences that their adaptations to altered CO<sub>2</sub> concentration have in terms of the ecosystem they inhabit. The presence of leaf gas films, lack of tissue porosity or other morphological traits of the leaf, as well as photochemical differences and biochemical responses to the imposed condition, are very important characteristics that from a holistic point of view have enormous impacts on the estuarine water column chemistry as a habitat for heterotrophic species. Salt marshes will play a crucial role in counterbalancing the effects of climate change, in terms of water column oxygenation and in buffering its acidification by withdrawing excess CO<sub>2</sub>.

## Sources of Funding

The work was funded by ‘Fundação para a Ciência e Tecnologia (FCT)’ at the Centre of Oceanography (CO) throughout the project PEst-OE/MAR/UI0199/2011, the Institute of Marine Research (IMAR) throughout the project PEst-C/MAR/UI0284/2011 and this specific work throughout the ECOSAM project (PTDC/AAC-CLI/104085/2008). The investigation of B.D. was supported by FCT through a PhD grant (SFRH/BD/75951/2011).

## Contributions by the Authors

In the present work, all the authors were involved according to their area of expertise. B.D. was responsible for the biophysical and photochemical analyses and D.S. for the antioxidant enzymatic assays. I.C. and J.C.M. were responsible for the supervision of the work and for the final corrections and suggestions in data interpretation.

H.S. and N.S. supervised the work and introduced their expertise in terms of halophyte ecology.

## Conflicts of Interest Statement

None declared.

## Acknowledgements

The authors thank the ‘Fundação para a Ciência e Tecnologia (FCT)’ for funding the research at the Centre of Oceanography (CO) throughout the project PEst-OE/MAR/UI0199/2011, the Institute of Marine Research (IMAR) throughout the project PEst-C/MAR/UI0284/2011 and this specific work throughout the ECOSAM project (PTDC/AAC-CLI/104085/2008).

## Literature Cited

- Andersen T, Pedersen O. 2002. Interactions between light and CO<sub>2</sub> enhance the growth of *Riccia fluitans*. *Hydrobiologia* **477**: 163–170.
- Bailey-Serres J, Voesenek L. 2008. Flooding stress: acclimations and genetic diversity. *Annual Review of Plant Biology* **59**:313–339.
- Beer S, Ilan M, Eshel A, Weil A, Brickner I. 1998a. The use of pulse amplitude modulated (PAM) fluorometry for *in situ* measurements of photosynthesis in two Red Sea Faviid corals. *Marine Biology* **131**:607–612.
- Beer S, Vilenkin B, Weil A, Veste M, Susel L, Eshel A. 1998b. Measuring photosynthesis in seagrasses by pulse amplitude modulated (PAM) fluorometry. *Marine Ecology Progress Series* **174**:293–300.
- Bergmeyer HU, Gawehn K, Grassl M. 1974. Enzymes as biochemical reagents. In: Bergmeyer HU, ed. *Methods in enzymatic analysis*. New York: Academic Press, 425–522.
- Bowes G. 1993. Facing the inevitable: plants and increasing atmospheric CO<sub>2</sub>. *Annual Review of Plant Physiology and Plant Molecular Biology* **44**:309–332.
- Bradford M. 1976. A rapid and sensitive method for the quantification of microgram quantities of protein utilizing the principle of protein-dye-binding. *Analytical Biochemistry* **72**:248–254.
- Caçador I, Tibério S, Cabral H. 2007. Species zonation in Corroios salt marsh in the Tagus estuary (Portugal) and its dynamics in the past fifty years. *Hydrobiologia* **587**:205–211.
- Caçador I, Caetano M, Duarte M, Vale C. 2009. Stock and losses of trace metals from salt marsh plants. *Marine Environmental Research* **67**:75–82.
- Caçador I, Neto JM, Duarte B, Barroso DV, Pinto M, Marques JC. 2013. Development of an angiosperm quality assessment index (AQuA—index) for ecological quality evaluation of Portuguese water bodies—a multi-metric approach. *Ecological Indicators* **25**:141–148.
- Colmer T, Pedersen O. 2008. Underwater photosynthesis and respiration in leaves of submerged wetland plants: gas films improve CO<sub>2</sub> and O<sub>2</sub> exchange. *New Phytologist* **177**:918–926.
- Colmer T, Voesenek L. 2009. Flooding tolerance: suites of plant traits in variable environments. *Functional Plant Biology* **36**:665–681.
- Duarte B, Raposo P, Caçador I. 2009. *Spartina maritima* (cordgrass) rhizosediment extracellular enzymatic activity and its role on



- organic matter decomposition and metal speciation processes. *Marine Ecology* **30**:65–73.
- Duarte B, Caetano M, Almeida P, Vale C, Caçador I. 2010. Accumulation and biological cycling of heavy metal in the root–sediment system of four salt marsh species, from Tagus estuary (Portugal). *Environmental Pollution* **158**:1661–1668.
- Duarte B, Silva V, Caçador I. 2012. Hexavalent chromium reduction, uptake and oxidative biomarkers in *Halimione portulacoides*. *Ecotoxicology and Environmental Safety* **83**:1–7.
- Duarte B, Santos D, Marques JC, Caçador I. 2013a. Ecophysiological adaptations of two halophytes to salt stress: photosynthesis, PS II photochemistry and anti-oxidant feedback—implications for resilience in climate change. *Plant Physiology and Biochemistry* **67**:178–188.
- Duarte B, Couto T, Freitas J, Valentim J, Silva H, Marques JC, Caçador I. 2013b. Abiotic modulation of *Spartina maritima* photosynthetic ecotypic variations in different latitudinal populations. *Estuarine, Coastal and Shelf Science* **130**:127–137.
- Duarte B, Santos D, Silva H, Marques JC, Caçador I. 2014a. Photochemical and biophysical feedbacks of C<sub>3</sub> and C<sub>4</sub> Mediterranean halophytes to atmospheric CO<sub>2</sub> enrichment confirmed by their stable isotope signatures. *Plant Physiology and Biochemistry* **80**:10–22.
- Duarte B, Santos D, Marques JC, Caçador I. 2014b. Biophysical probing of *Spartina maritima* photosystem II changes during increased submersion periods: possible adaptation to sea level rise. *Plant Physiology and Biochemistry* **77**:122–132.
- Duarte B, Silva G, Costa JL, Medeiros JP, Azeda C, Sá E, Metelo I, Costa MJ, Caçador I. 2014c. Heavy metal distribution and partitioning in the vicinity of the discharge areas of Lisbon drainage basins (Tagus Estuary, Portugal). *Journal of Sea Research* **93**:101–111.
- Furbank RT. 1998. C<sub>4</sub> pathway. In: Raghavendra AS, ed. *Photosynthesis, a comprehensive treatise*. Cambridge, UK: Cambridge University Press, 123–135.
- Geissler H, Hussin S, Koyro H-W. 2009. Elevated atmospheric CO<sub>2</sub> concentration ameliorates effects of NaCl salinity on photosynthesis and leaf structure of *Aster tripolium* L. *Journal of Experimental Botany* **60**:137–151.
- Genty B, Briantais J-M, Baker N. 1989. The relationship between the quantum yield of photosynthetic electron transport and quenching of chlorophyll fluorescence. *Biochimica et Biophysica Acta* **990**:87–92.
- Grossi V, Raphael D. 2003. Long-chain (C<sub>19</sub>–C<sub>29</sub>) 1-chloro-*n*-alkanes in leaf waxes of halophytes of the Chenopodiaceae. *Phytochemistry* **63**:693–698.
- IPCC. 2002. Climate change and biodiversity. IPCC technical paper V. Contribution of the Working Group II to the fourth assessment report of the Intergovernmental Panel on Climate Change.
- Keeley JE. 1998. Photosynthetic pathway diversity in a seasonal pool community. *Functional Ecology* **13**:106–118.
- Lorimer GH. 1981. The carboxylation and oxygenation of ribulose-1,5-bisphosphate carboxylase: the primary event in photosynthesis and photorespiration. *Annual Review of Plant Physiology* **32**:349–383.
- Marklund S, Marklund G. 1974. Involvement of superoxide anion radical in the autoxidation of pyrogallol and a convenient assay for superoxide dismutase. *European Journal of Biochemistry* **47**:464–469.
- Marshall HJ, Geider RJ, Flynn KJ. 2000. A mechanistic model of photoinhibition. *New Phytologist* **145**:347–359.
- Mendelssohn I, Morris J. 2000. *Ecophysiological controls on the productivity of Spartina alterniflora Loisel in concepts and controversies in tidal marsh ecology*. The Netherlands: Springer, 59–80.
- Mommer L, Wolters-Arts M, Andersen C, Visser EJW, Pedersen O. 2007. Submergence-induced leaf acclimation in terrestrial species varying in flooding tolerance. *New Phytologist* **176**:337–345.
- Panda D, Rao DN, Sharma SG, Strasser RJ, Sarkar RK. 2006. Submergence effects on rice genotypes during seedling stage: probing of submergence driven changes of photosystem 2 by chlorophyll a fluorescence induction O–J–I–P transients. *Photosynthetica* **44**:69–75.
- Pedersen O, Colmer T. 2006. Oxygen dynamics during submergence in the halophytic stem succulent *Halosarcia pergranulata*. *Plant, Cell and Environment* **29**:1389–1399.
- Pedersen O, Rich SM, Colmer TD. 2009. Surviving floods: leaf gas films improve O<sub>2</sub> and CO<sub>2</sub> exchange, root aeration, and growth of completely submerged rice. *The Plant Journal* **58**:147–156.
- Pedersen O, Malik A, Colmer T. 2010. Submergence tolerance of *Hordeum marinum*: dissolved CO<sub>2</sub> determines underwater photosynthesis and growth. *Functional Plant Biology* **37**:524–531.
- Platt T, Gallegos CL, Harrison WG. 1980. Photoinhibition of photosynthesis in natural assemblages of marine phytoplankton. *Journal of Marine Research* **38**:687–701.
- Ram PC, Singh AK, Singh BB, Singh VK, Singh HP, Setter TL, Singh VP, Singh RK. 1999. Environmental characterization of floodwater in Eastern India: relevance to submergence tolerance of lowland rice. *Experimental Agriculture* **35**:141–152.
- Raven JA. 1970. Exogenous inorganic carbon sources in plant photosynthesis. *Biological Reviews* **45**:167–221.
- Raven JA. 1972. Endogenous inorganic carbon sources in plant photosynthesis. II. Comparison of total CO<sub>2</sub> production in the light with measured CO<sub>2</sub> evolution in the light. *New Phytologist* **71**:995–1014.
- Runcie JW, Durako MJ. 2004. Among-shoot variability and leaf-specific absorbance characteristics affect diel estimates of *in situ* electron transport of *Posidonia australis*. *Aquatic Botany* **80**:209–220.
- Sand-Jensen K. 1989. Environmental variables and their effect on photosynthesis of aquatic plant communities. General features to aquatic photosynthesis. *Aquatic Botany* **34**:5–25.
- Sand-Jensen K, Pedersen MF, Nielsen SL. 1992. Photosynthetic use of inorganic carbon among primary and secondary water plants in streams. *Freshwater Biology* **27**:283–293.
- Serôdio J., Catarino F. 2000. Modelling the primary production of intertidal microphytobenthos: time scales of variability and effects of migratory rhythms. *Marine Ecology Progress Series* **192**:13–30.
- Setter TL, Waters I, Wallace I, Bhekasut P, Greenway H. 1989. Submergence of rice I. Growth and photosynthetic response to CO<sub>2</sub> enrichment of floodwater. *Australian Journal of Plant Physiology* **16**:251–263.
- Smith F, Walker N. 1980. Photosynthesis by aquatic plants: effects of unstirred layers in relation to assimilation of CO<sub>2</sub> and HCO<sub>3</sub><sup>–</sup> and to carbon isotopic discrimination. *New Phytologist* **86**:245–259.

- Strasser RJ, Stirbet AD. 2001. Estimation of the energetic connectivity of PS II centres in plants using the fluorescence rise O–J–I–P. Fitting of experimental data to three different PS II models. *Mathematics and Computers in Simulation* **56**:451–461.
- Taiz L, Zeiger E. 2002. *Plant physiology*. 3rd ed. Sunderland, MA: Sinauer Associates, Inc., Publishers.
- Teranishi Y, Tanaka A, Osumi M, Fukui S. 1974. Catalase activities of hydrocarbon-utilizing *Candida* yeast. *Agricultural and Biological Chemistry* **38**:1213–1220.
- Tiryakioglu M, Eker S, Ozkutlu F, Husted S, Cakmak I. 2006. Antioxidant defence system and cadmium uptake in barley genotypes differing in cadmium tolerance. *Journal of Trace Elements in Medicine and Biology* **20**:181–189.
- Urano K, Kurihara Y, Motoaki S, Shinozaki K. 2010. ‘Omics’ analyses of regulatory networks in plant abiotic stress responses. *Current Opinion in Plant Biology* **13**:132–138.
- Voesenek L, Rijnders J, Peeters A, van de Steeg H, Kroon H. 2004. Plant hormones regulate fast shoot elongation under water: from genes to communities. *Ecology* **85**:16–27.
- Voss I, Sunil B, Scheibe R, Raghavendra S. 2013. Emerging concept for the role of photorespiration as an important part of abiotic stress response. *Plant Biology* **15**:713–722.
- Wagner P, Furstner R, Barthlott W. 2003. Quantitative assessment to the structural basis of water repellency in natural and technical surfaces. *Journal of Experimental Botany* **54**:1295–1303.
- Waters I, Armstrong W, Thomson CJ, Setter TL, Adkins S, Gibbs J, Greenway H. 1989. Diurnal changes in radial oxygen loss and ethanol metabolism in roots of submerged and non-submerged rice seedlings. *New Phytologist* **113**:439–451.
- Yamaguchi-Shinozaki K, Shinozaki K. 2006. Transcriptional regulatory networks in cellular responses and tolerance to dehydration and cold stresses. *Annual Review of Plant Biology* **57**:781–803.
- Zhu XG, Govindjee, Baker NR, Sturler ED, Ort DR, Long SP. 2005. Chlorophyll a fluorescence induction kinetics in leaves predicted from a model describing each discrete step of excitation energy and electron transfer associated with Photosystem II. *Planta* **223**:114–133.